

Laser Interferometry for Broad Area SPR-Grating Couplers in Chemical Applications [†]

Mauricio Moreno-Sereno ^{1,2,*}, Noemi Pérez ³, Guillem Domenech-Gil ^{1,2},
Laura Parellada-Monreal ⁴, Miguel Martínez-Calderón ⁴, Mikel Gómez-Aranzadi ⁴,
Nasser Darwish ^{1,5}, Gemma G. Mandayo ⁴ and Albert Romano-Rodríguez ^{1,2}

¹ Institute of Nanoscience and Nanotechnology (IN2UB), Universitat de Barcelona (UB),
c/Martí i Franquès 1, E-08028 Barcelona, Spain; guillemdom@gmail.com (G.D.-G.);
nasser.darwish@gmail.com (N.D.); aromano@el.ub.edu (A.R.-R.)

² Department of Electronics, Universitat de Barcelona (UB), c/Martí i Franquès 1, E-08028 Barcelona, Spain

³ Universidad de Navarra, Department of Electrical, Electronic and Automatic Engineering, Tecnun,
Pº de Manuel Lardizabal 13, 20018 Donostia-San Sebastián. Gipuzkoa, Spain; nperez@tecnun.es

⁴ Ceit and Tecnun, Universidad de Navarra, Department of Transport and Energy,
Pº de Manuel Lardizabal 13, 20018 Donostia-San Sebastián. Gipuzkoa, Spain; lparellada@ceit.es (L.P.-M.);
mmcalderon@ceit.es (M.M.-C.); mgomez@ceit.es (M.G.-A.); ggmandayo@ceit.es (G.G.M.);

⁵ Institute of Science and Technology, AM Campus 1, A-3400 Klosterneuburg, Austria

* Correspondence: mmoreno@el.ub.edu, Tel.: +34-934-039-150

[†] Presented at the EuroSensors 2017 Conference, Paris, France, 3–6 September 2017.

Published: 28 August 2017

Abstract: In this work, the fabrication of a SPR (Surface Plasmon Resonance)-grating coupler using Laser Interference Lithography (LIL) has been investigated, giving rise to large area diffraction gratings on a 100 nm-thick gold film. The period of the diffraction grating is $\Lambda = 500$ nm. The SPR sensor has been tested towards several liquids showing a maximum sensitivity of $S = 390$ nm/RIU.

Keywords: Laser Interference Lithography; grating; Surface Plasmon Resonance; chemical sensor

1. Introduction

SP (Surface Plasmons) are surface electromagnetic waves along a metal/dielectric interface. The real part of the dielectric constant of the metal must be negative, as in gold, silver or aluminum. For biological applications, gold is the most used metal due to the high control of interaction of this metal's surface with a large number of biochemical species that can be adhered to it. As there is no need of fluorescent markers, this technique is classified as label-free.

In the Kretschmann's configuration [1], the evanescent field of total internal reflection in the base of a prism can couple and excite Surface Plasmon (SP) at the substrate-metal interface. A second approach is the use of diffraction of light on a diffraction grating patterned on the gold layer. The diffracted wave excites a SP if the projection of the propagation constant matches that of the SP evanescent wave. This second technique does not need a prism nor the mechanical pressure system. The drawback is the necessity of fabricating a diffraction grating in where the prism setup uses a planar gold layer. The period needed for these grating require nanolithography techniques.

Electron Beam Lithography (EBL) is suitable for prototyping nanostructured surfaces in an area of few mm². The patterns are transferred sequentially by an electron beam to an electron-sensitive resist. After developing the resist, the metal can be etched by different means, resulting in the transfer of the designed pattern to the metal layer. Time and costs increase linearly with the size of the patterned area. In contrast, Laser Interference Lithography (LIL) exposes large surface at once, resulting in larger areas (about 1 cm²) and a much better cost-effectiveness. Similar to EBL, after developing, an etching process is needed to transfer the periodic pattern to the metal.

2. Materials and Methods

2.1. Fabrication Process

On a fused silica substrate, a 5 nm-thick Ti film is first deposited by sputtering as adhesion layer, followed by sputtered gold film, so the total metal thickness is 100 nm. Next, a 300 nm-thick AZnLOF 2070 negative photoresist is spun. In order to pattern the photoresist, a two laser beam interference set-up is used with a frequency-tripled Nd:YAG laser source ($\lambda = 355$ nm). The photoresist is prebaked for 60 s at 100 °C and, then, exposed to a single pulse of 8 ns and a fluence of 15 mJ/cm² to obtain a 500 nm period grating. The sample is then postbaked at 110 °C for 60 s and developed in AZ-726 MIF developer (MicroChemicals GmbH, Ulm, Germany) for 20 s at 21 °C. Subsequently, it is immersed for 60 s in deionized water to stop the development process and, finally, dried with N₂.

In order to transfer the periodic pattern from the photoresist to the gold layer, a Reactive Ion Etching (RIE) equipment was used with a non-reactive recipe: in an environment of 20 sccm of Ar, RF power of 173 W was used for 20, 30 and 40 s (chamber conditions: 20 °C temperature and 10 mTorr pressure). Trenches 250 nm wide with two different deeps were obtained over a circular area of approximately 1 cm². In Figure 1a a photograph of the optical SPR-G sensor is shown, while Figure 1b is a detailed SEM micrograph of the etched grating. The LIL technique has been previously used by the authors in [2] for patterning diffraction gratings on Si₃N₄ and used as diffraction grating couplers also for optical biosensing purposes.

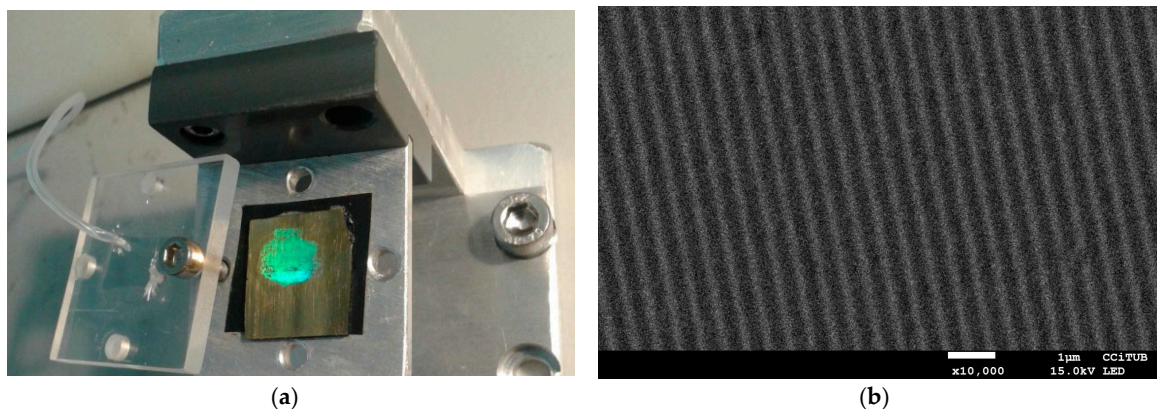


Figure 1. (a) Photograph of the area of the gold film patterned with a diffraction grating; (b) Scanning Electron Microscope photograph of the $\Lambda = 500$ nm period diffraction grating.

2.2. Instrumentation

Spectral interrogation has been used for characterization with a broadband source LS-1 and a spectrometer SD-2000, both from Ocean Optics, to measure the reflectivity of the SPR-G sensor [2]. LS-1 is prepared for operating with fiber optics and the light is collimated and divided with a beam-splitter, being one of the beams TM polarized and focused using a 4× OLYMPUS objective. After reflection in the sensor, the light from the objective is focused in another fiber towards the spectrometer. The reflected spectrum is normalized to a reference spectrum measured in a flat area on the optical sensor, where there is no diffraction grating.

Figure 2 presents a typical reflection spectrum, showing the dip at about 670 nm as result of the resonance. In cyan the raw spectrum is showed, while the blue corresponds to the smoothed signal, calculated to reduce noise, which is further processed with MATLAB™ to find the minimum.

The base of the sensor is fixed to two MT3/M translation stages from THORLABS, for an X and Y scanning of the sensor. The movement is produced with two low-cost linear actuator stepper from CROUZET™, with a 10 mm displacement, and a commercial driver motor board (TB6560). The latter is controlled with the popular MSP430 microcontroller from TEXAS™, which is connected to a PC. The result is a low cost platform with a resolution of 8 μm in X and Y directions.

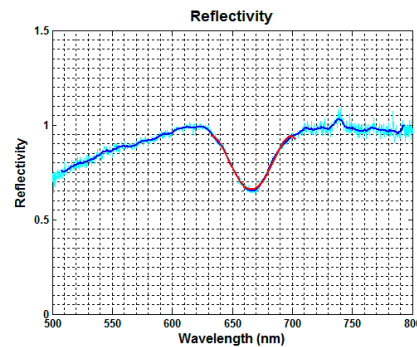


Figure 2. Typical reflectance spectrum showing a dip at $\lambda_{\text{DIP}} = 670$ nm. Cyan: raw data from spectrometer; blue: smoothed data, and red: fitted region to find the minimum.

3. Results

3.1. Optical Characterization

Figure 3 is a 2D representation of the value of the resonance wavelength (left) and the depth of the resonance dip (right). In this case the measurement is done in steps of 200 μm and the sensor is covered with water. The blue spots correspond to flat areas of the sensor and they are fixed to $\lambda_{\text{flat}} = 450$ nm in order to have a proper contrast in the graph.

In Figure 3 left, a small variation in the red tone at different points can be appreciated. The brighter red tone corresponds to lower wavelengths. The reason can be a non-uniformity of the grating depth at the different points. It seems that at the periphery of the laser spot the resonance wavelength decreases. Figure 4 show two histograms obtained from the results of Figure 3. The inner spots has a mean value of $\lambda_{\text{inner}} = 695.4 \text{ nm} \pm 4 \text{ nm}$ and in the periphery $\lambda_{\text{outer}} = 678.1 \text{ nm} \pm 4.6 \text{ nm}$.

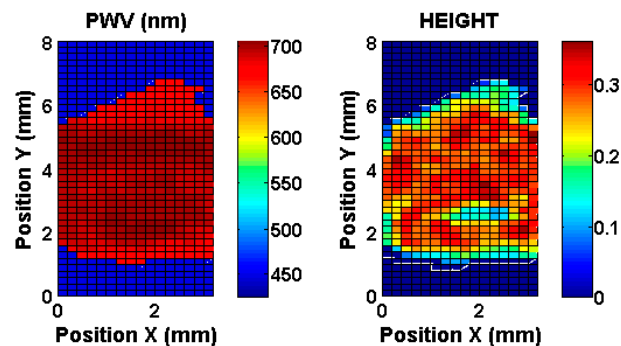


Figure 3. Left: Resonance wavelength in function of the (x, y) position; Right: the magnitude or depth of the resonant dip. The sensor is covered with water.

3.2. Bulk Characterization

In this section, we present the results of the characterization of the SPRG sensors under the presence of different liquids in order to obtain their bulk sensitivity. Figures 3 and 4 are a particular case for water. The sensor is inside a fluidic chamber made of PDMS gasket and a top methacrylate cover. The system makes the X-Y scan of the surface, measures the spectrum at every position and finally calculates the statistics of the resonant wavelength.

Figure 5 is the result of the resonance wavelength for water ($n = 1.33$), isopropanol ($n = 1.38$) and glycerol ($n = 1.48$), for two SPRG sensors with different etching times. The resonance represented is the mean value of the grating surface scanned, without taking into account the periphery or center of the grating. The slope of the fitted line is the bulk sensitivity, which is around of $S = 387 \text{ nm/RIU}$ for 100 s etching time and $S = 354 \text{ nm/RIU}$ for 60 s etching time. The mean resolution of the SD2000 spectrometer is around $\Delta\lambda = 0.3 \text{ nm}$, but a post processing allows lowering it to 0.01 nm, and then, a refractometric resolution of $2.7 \times 10^{-5} \text{ RIU}$ is expected.

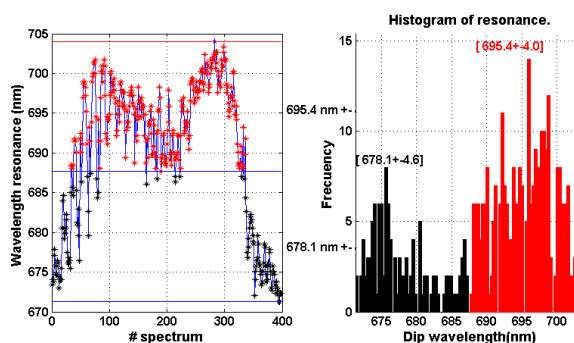


Figure 4. Left: Resonance wavelength along the zigzag scanning. Right: Histogram of the resonance wavelength for the measurement of Figure 3. The values marked in red correspond to the inner locations of the sensor while the black ones correspond to the periphery.

The sensitivity presents an excellent value but lower in front to other structures with plastic substrate, as $S = 751 \text{ nm/RIU}$ [3]. From these results, it seems that shallower etching for a gold thickness of 100 nm is best, but this must be confirmed in future simulations with FDTD analysis.

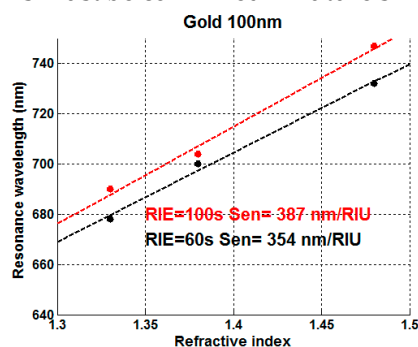


Figure 5. Bulk sensitivity for SPRG sensors. Black: 60 s of RIE etching; Red: 100 s RIE etching.

4. Conclusions

In this work, the capabilities of LIL technique for rapid nano structuration of a large area of gold (around 1 cm^2) and the possibility of its use as chemical sensor have been shown. We have developed a low-cost platform that can scan the surface of the sensor with a resolution of $\Delta x = \Delta y = 8 \mu\text{m}$. The best bulk sensitivity obtained for the SPRG sensors is around 390 nm/RIU.

Acknowledgments: This research has been founded by the Spanish Government through the projects TEC2009-12543 and TEC2013-48147-C6-1-R (AEI/FEDER, EU) and the Basque Government through the Elkartek program (MICRO4FAB grant n°. KK-2016-00030).

Conflicts of Interest: The authors declare no conflicts of interest.

References

1. Homola, J. (Volume Ed.) *Surface Plasmon Resonance Based Sensors*; Series on Chemical Sensors and Biosensors: Methods and Applications; Springer: Berlin/Heidelberg, Germany, 2006.
2. Rodríguez-Franco, P.; Arriola, A.; Darwish, N.; Jaramillo, J.J.; Keshmiri, H.; Tavera, T.; Olaizola S.M.; Moreno, M. Fabrication of broad area optical nanostructures for high throughput chemical sensing. *Sens. Actuators B Chem.* **2013**, *187*, 356–362. <https://doi.org/10.1016/j.snb.2012.12.039>
3. Kumari, S.; Mohapatra, S.; Moirangthem, R.S. Nano-imprint gold grating as refractive index sensor. *AIP Conf. Proc.* **2016**, *1728*, 020539, doi:10.1063/1.4946590.

